CHEMISTRY
A European Journal

A Journal of
ChemPubSoc Europe

Accepted Article

Title: Buttressing effect as key design principle towards highly efficient palladium/N-heterocyclic carbene Buchwald-Hartwig amination catalysts

Authors: Yin Zhang, Guy Lavigne, Noël Lugan, and Vincent César

To be cited as: *Chem. Eur. J.* 10.1002/chem.201702859

Link to VoR: http://dx.doi.org/10.1002/chem.201702859

Supported by
ACES

WILEY-VCH

10.1002/chem.201702859

WILEY-VCH

FULL PAPER

Buttressing effect as key design principle towards highly efficient palladium/N-heterocyclic carbene Buchwald-Hartwig amination catalysts

Yin Zhang,[a] Guy Lavigne†,[a] Noël Lugan,[a] Vincent César*,[a]

Abstract: The backbone substitution of the standard 1,3-bis(2,6-diisopropylphenyl)-2*H*-imidazol-2-ylidene (IPr) ligand by dimethylamino groups was previously shown to induce a dramatic improvement of the catalytic efficiency of the corresponding Pd-PEPPSI pre-catalysts in N-arylation reaction. A thorough structure/activity study aiming at rationalizing this beneficial effect is now described. In addition to the previously reported IPr^{NMe_2} and $IPr^{(NMe_2)_2}$ ligands, the new IPr^{NiPr_2} and $IPr^{(NMe_2,Cl)}$ ligands bearing respectively, one bulkier diisopropylamino group and a combination of dimethylamino and chloro substituents, have been designed and included in the study. It is shown that the influence of the backbone-substitution is actually steric in origin and is related to the well-known buttressing effect encountered in arene chemistry. The usefulness and versatility of this approach are demonstrated through the development of a highly efficient catalytic system for the challenging arylation of bulky α,α,α-trisubstituted primary amines. The optimized system based on the [PdCl(η^3-cinnamyl)($IPr^{(NMe_2)_2}$)] or [PdCl(η^3-cinnamyl)(IPr^{NiPr_2})] pre-catalysts operates under unprecedented mild conditions (catalyst loadings: 0.5-2 mol%, reaction temperatures: 40-60°C) and over a large substrate scope.

Introduction

The palladium-catalyzed amination of aryl halides has become a valuable and powerful tool for the construction of carbon-nitrogen (C-N) bonds to access anilines, a common structure found in natural compounds, drug agents, fine chemicals and other complex molecules.[1,2] The broad success of this catalysis has greatly benefited from *i*) the development of well-defined, easy to handle pre-catalysts able to readily liberate the mono-ligated palladium(0) active species into the catalytic cycle,[3] and especially from *ii*) the advent of specially designed classes of ligands, enabling the C-N coupling in high levels of efficiency and selectivity. In that prospect, and apart bulky monodentate and electron-rich tertiary phosphines,[4] N-heterocyclic carbenes (NHCs)[5,6] have been increasingly employed as ancillary ligands to provide highly stable and active Pd-NHC catalysts thanks to their strong σ-electronic donation and good steric protection.[7] Another beneficial advantage of NHCs resides in the high synthetic flexibility of their precursors, offering in fine a wide scope of stereoelectronic properties for the corresponding ligands.[8]

During the last decade, collective efforts have been directed towards the improvement of Pd-NHC based catalytic systems in terms of efficiency, scope and practicability. From the benchmark 1,3-bis(2,6-diisopropylphenyl)-2*H*-imidazol-2-ylidene ligand (IPr), which led to the best catalytic outcome among the classical NHCs,[9] excellent results have been obtained upon formal replacement of the 2,6-diisopropylphenyl (Dipp) nitrogen substituents by bulkier aryl groups bearing extended ortho substituents such as 3-pentyl (leading to the IPent ligand),[10] 4-heptyl (IHept ligand),[11] 5-nonyl (INon ligand)[11] or diphenylmethyl groups (IPr* ligand) (Fig. 1).[12] The development of these NHCs was based on the concept of "flexible steric bulk", first introduced by Glorius, according to which the bulky NHC ligand efficiently stabilizes the reactive, mono-coordinated, low-valent active species [Pd^0(NHC)] and facilitates the reductive elimination step, while its flexibility allows its adjustment to the incoming substrates.[13] In parallel, we and others have investigated the direct modification of the heterocyclic skeleton of the IPr ligand and have shown that backbone substitution has eventually a beneficial effect on the catalytic efficiency of the resulting Pd-catalysts.[14,15] The improvement was particularly impressive when substituting the 4/5 positions of the imidazolyl ring with one (IPr^{NMe_2}) and especially with two dimethylamino groups ($IPr^{(NMe_2)_2}$).[14a-b] In our first report, we concluded that this observed booster effect could be seen as the result of a synergism between steric and electronic effects since the incorporation of the NMe_2 groups led to a sequential increase of both the electronic donation and steric bulkiness of the correspondi ng NHC. In the meantime, Organ and co-workers developed a wide variety of Pd-PEPPSI-NHC pre-catalysts,[16] some of the NHCs exhibiting backbone modification, and showed in particular that pre-catalysts based on the dichloro-substituted $IPent^{Cl_2}$ or $IHept^{Cl_2}$ supporting ligands greatly outperform their respective IPent-and IHept-based standard analogues.[17,18] In these studies, the improvement of the pre-catalysts efficiency was essentially ascribed to steric effects, while electronic effects were judged as being rather unimportant.[17b,c]

[a] Dr Y. Zhang, Dr G. Lavigne, Dr N. Lugan, Dr V. César
LCC-CNRS, Université de Toulouse, INPT, UPS, Toulouse, France
Fax: (+)33 (0) 5 61 55 30 03
E-mail: vincent.cesar@lcc-toulouse.fr
† Deceased on 23 April 2015

Supporting information for this article is given via a link at the end of the document

10.1002/chem.201702859
WILEY-VCH

FULL PAPER

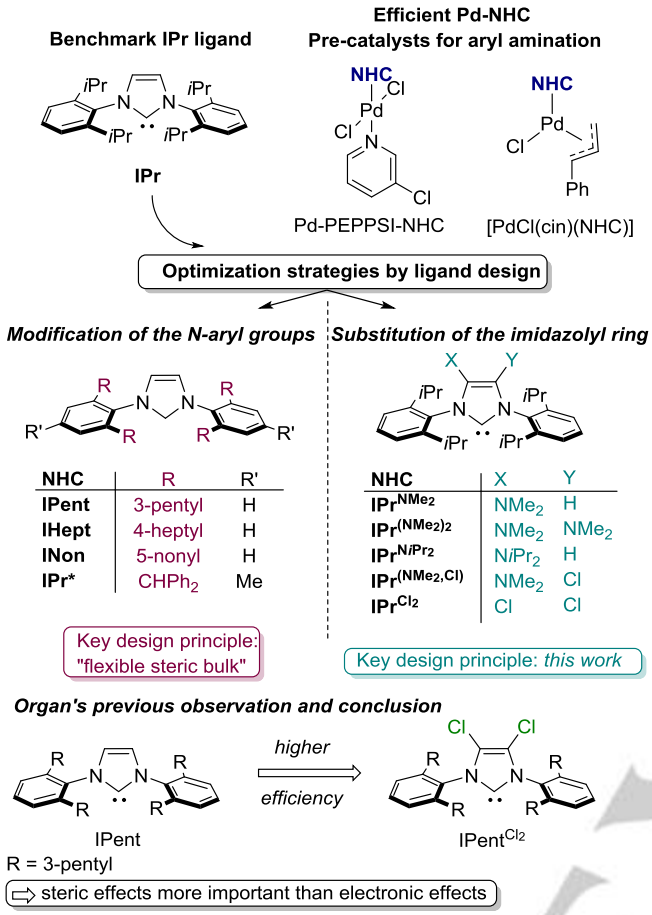

Figure 1. Context and principle of the present work.

In this context, we became interested in getting a deeper understanding of the structural features at play in our systems and, eventually, in establishing the "key design principle" on which optimization of Pd-NHC catalysts through backbone functionalization may be based. To this end, our strategy relied on further derivatizing our first two amino-substituted NHC ligands IPr^{NMe_2} and $IPr^{(NMe_2)_2}$ into two complementary directions: *i*) a formal substitution of the dimethylamino (NMe_2) group by the bulkier diisopropylamino ($NiPr_2$) group in order to increase steric shielding and conversely, *ii*) a formal replacement of one of the dimethylamino groups by an electron-withdrawing chlorine atom in order to diminish the electronic donicity.

Through the present work, we shall demonstrate that the observed beneficial influence of the substitution of the imidazolylidene ring on the catalytic activity in Pd-catalyzed amination mainly arises from steric effects prompting us to formalize it as a buttressing effect, which is classically encountered in aryl chemistry. Exploiting this concept allowed to develop a highly efficient Pd-NHC catalytic system for the challenging arylation of bulky primary amines.

Results and Discussion

Synthesis of the new NHCs and palladium PEPPSI pre-catalysts

The 4-(diisopropylamino)imidazolium triflates **3a-b**^{NiPr_2} were prepared following the same strategy than the one we previously developed for the 4-(dimethylamino) imidazolium triflates **3a-b**^{NMe_2}.[14a] The two-step sequence consists in an alkylation of the formamidine **1a-b** with N,N-diisopropyl-2-chloroacetamide followed by a selective activation of the amide function of the intermediate **2a-b** by triflic anhydride leading to an intramolecular cyclization (Scheme 1). Whereas the first step proceeded in high yield (95-99%), the second cyclisation step was less efficient as compared to the dimethylamino derivatives, probably due to a higher steric congestion of the heterocycle. The corresponding Pd-PEPPSI-IPr^{NiPr_2} complex **5**^{NiPr_2} was obtained in four steps through the classical route we described in our previous communication.[14a] Complex **5**^{NiPr_2} was fully characterized by the usual spectroscopic methods supplemented by a single-crystal X-Ray diffraction study (Figure 2).

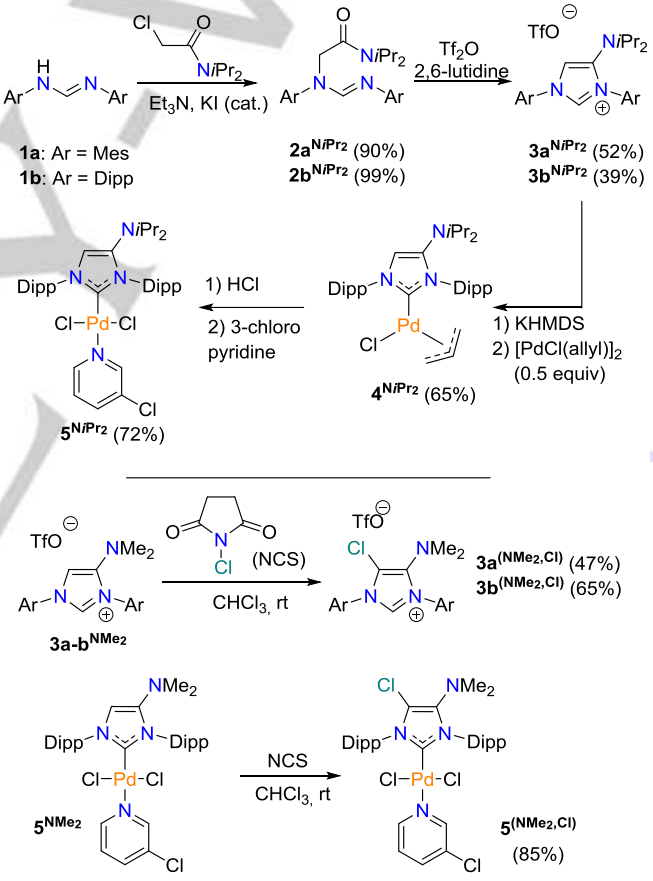

Scheme 1. Synthesis of the imidazolium salts **2a-b**$^{N/Pr2}$, and **2a-b**$^{(NMe2,Cl)}$ and of the corresponding Pd-PEPPSI complexes **3**^{NiPr2}, and **3**$^{(NMe2,Cl)}$ (Mes = 2,4,6-trimethylphenyl, Dipp = 2,6-diisopropylphenyl).

We next turned our attention to the synthesis of the imidazolium salts **3a-b**$^{(NMe_2,Cl)}$ through direct oxidative chlorination of the corresponding imidazolium salts **3a-b**^{NMe_2} on the imidazolyl C5

10.1002/chem.201702859

position (Scheme 1). We were encouraged in this direction by our previous demonstration of such a reactivity trend in related NHCs having a functionalized heterocyclic backbone.[19] Whereas no reaction occurred when mixing the imidazolium triflates **3a-b**^{NMe_2} with a small excess (1.2 equiv) of N-chlorosuccinimide (NCS) in CH_2Cl_2 at room temperature, we were pleased to observe the complete disappearance of the signal corresponding to the C5-proton of the imidazolium ring in the ^{1}H NMR spectrum after only 30 minutes when carrying out the reaction in $CHCl_3$. This dichotomy in reactivity could be ascribed to the more acidic character of chloroform, which should assist this transformation. The pure imidazolium triflates **3a-b**$^{(NMe_2,Cl)}$ were obtained in 47-65% yields after a simple column chromatography and/or recrystallization. The molecular structure of **3b**$^{(NMe_2,Cl)}$ was further confirmed by an X-Ray diffraction analysis (Figure S1, supporting information). Such a reactivity is unique as previous procedures for the halogenation of imidazolium rings all proceeded in three steps involving the generation of the free imidazol-2-ylidene, its reaction with an oxidizing reagent, and a final reprotonation. Besides, strict anhydrous and inert reaction conditions are also required limiting the practicability and generality of the previous procedure.[20] Moreover, we could also capitalized on the peculiar reactivity of the 4-(dimethylamino)imidazol-2-ylidene core to directly derivatize the Pd-PEPPSI-IPr^{NMe_2} complex **5**^{NMe_2} into its chloro-derivative Pd-PEPPSI-IPr$^{(NMe_2,Cl)}$, **5**$^{(NMe_2,Cl)}$, in a very good yield (85%) (Scheme 1). This strategy turned out to be very advantageous for a rapid optimization of the catalytic system thanks to the late point of divergence.[19c-d,21] Complex **5**$^{(NMe_2,Cl)}$ was fully characterized and its molecular structure was unambiguously confirmed by an X-Ray diffraction analysis (Figure 2).

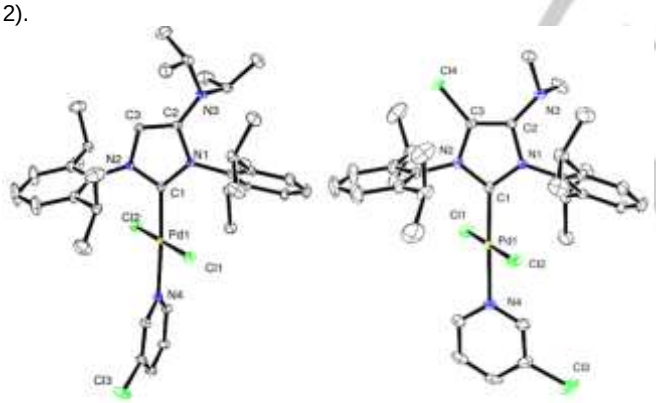

Figure 2. Molecular structures of **5**^{NiPr_2} (left) and **5**$^{(NMe_2,Cl)}$ (right), thermal ellipsoids set at the 30% probability level. H-atoms have been omitted for clarity.

Comparison of the catalytic activities of Pd-PEPPSI-NHC pre-catalysts

The catalytic efficiencies of the newly synthesized IPr-derived palladium PEPPSI pre-catalysts **5**^{NiPr_2} and **5**$^{(NMe_2,Cl)}$ were then evaluated in relation to those of our previously reported pre-catalysts **5**^{NMe_2} and **5**$^{(NMe_2)_2}$, of the standard Pd-PEPPSI-IPr pre-catalyst **5**, and of the dichloro-substituted **5**^{Cl_2}. For comparative purposes, the Pd-PEPPSI-IPent complex **6** was also included in this study. In a first set of experiments, the amination of 4-chloroanisole by morpholine (0.5 mol% catalyst, 1.1 eq. KO*t*Bu, DME, 25°C) was monitored against reaction time. The resulting reactivity profiles are displayed in Figure 3. In order to exclude potential experimental bias resulting from the variable hydrolysis level of the KO*t*Bu base, the latter was strictly purified to remove any traces of KOH and *t*BuOH, and then stored and weighed in a glove box. It is worth noting that this protocol drastically increases the catalytic efficiencies of all the pre-catalysts, including those of **5**^{NMe_2} and **5**$^{(NMe_2)_2}$ we investigated previously.[14a] As a matter of example, pre-catalyst **5**$^{(NMe_2)_2}$ led to full conversion in 10 minutes using the new protocol, to be compared to 2 hours using the previous one. Analysis of the kinetic curves indicates that the three pre-catalysts **5**$^{(NMe_2)_2}$, **5**$^{(NMe_2,Cl)}$, and **5**^{NiPr_2} exhibit about the same activity, while the IPent-derived complex **6** is a little less efficient. Conversely, the reaction did not reach completion after 2 hours when using pre-catalysts **5**^{NMe_2}, **5**, and **5**^{Cl_2}.

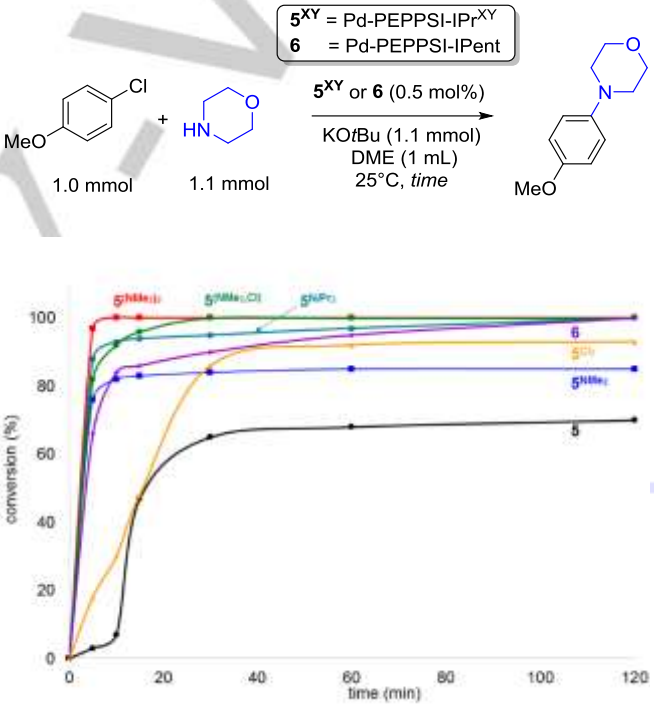

Figure 3. Reactivity profiles of the amination of 4-chloroanisole with morpholine using Pd-PEPPSI-NHC pre-catalysts **5**^{XY} and **6**. Conversions were determined by GC analysis using dodecane as internal standard. Reactions were performed in duplicate. DME = 1,2-dimethoxyethane.

We then decided to further explore the effect of the imidazolyl-backbone substitution in the challenging amination of the more sterically hindered 2-chloroanisole with morpholine under the same reaction conditions as above (Figure 4). The kinetic profiles revealed exactly the same trend as for 4-chloroanisole and is even accentuated. Indeed, complex **5**$^{(NMe_2)_2}$ shows the best efficiency with 91% conversion in 5 min, and full conversion after less than 1 hour, at 25°C. This result advantageously compares with the most active system known to date based on the [PdCl(cin)(SIPr)] pre-catalyst (cin = η^3-cinnamyl).[15a] Pre-

10.1002/chem.201702859

FULL PAPER

catalysts $\mathbf{5}^{NMe_2}$, and **5** are much less efficient showing 34%, and 15% conversion, respectively, after 2 hours, while $\mathbf{5}^{Cl_2}$ is basically inactive. Again, the pre-catalyst $\mathbf{5}^{NiPr_2}$ showing 90% conversion after 2 hours, is found to be much more efficient than its dimethylamino analogue $\mathbf{5}^{NMe_2}$, indicating that the increase of the steric hindrance of the amino substituent has a significant effect on the catalytic outcome of the amination reactions. Likewise, the chloro-amino-substituted $\mathbf{5}^{(NMe_2,Cl)}$ exhibits about the same activity as $\mathbf{5}^{(NMe_2)_2}$ suggesting also that the replacement of one of the NMe_2 group in $IPr^{(NMe_2)_2}$ by a chlorine atom has only a small effect in these two model catalyses. On the overall, the analysis of the two reactivity profiles allows classifying the various NHC ligands we considered into three categories according to the catalytic efficiency of the resulting pre-catalysts. The first category is composed of the most efficient $IPr^{(NMe_2)_2}$, $IPr^{(NMe_2,Cl)}$ and IPr^{NiPr_2} ligands, the third one includes the low efficiency IPr, IPr^{Cl_2} and IPr^{NMe_2} ligands, and the second one consisting of the IPent ligand only, its efficiency being in between.

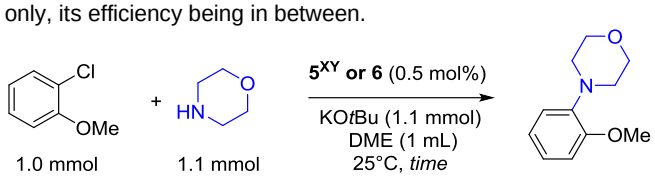

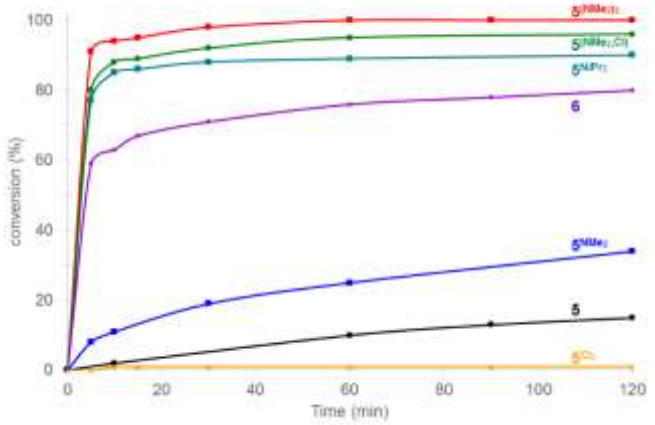

Figure 4. Reactivity profiles of the amination of 2-chloroanisole with morpholine using Pd-PEPPSI-NHC pre-catalysts $\mathbf{5}^{XY}$ and **6**. Conversions were determined by GC analysis using dodecane as internal standard. Reactions were performed in duplicate. DME = 1,2-dimethoxyethane.

Rationalization of the catalytic efficiency in terms of stereoelectronic effects: buttressing effect in N-heterocyclic carbenes

In order to investigate structure/activity trends, we then turned our attention to the in-depth characterization of stereoelectronic properties of the whole series of NHC ligands we had in hands. The overall electronic donicity of the NHC ligands were first quantified by recording the average IR stretching frequency ν_{CO}^{av} of the carbonyl ligands in complexes $[RhCl(CO)_2(IMes^{XY})]$ $\mathbf{8}^{XY}$, which is correlated to the Tolman Electronic Parameter (TEP) value of the ligand by a well-established linear correlation.[8b,c-22] The IMes platform was chosen here for comparison purposes with literature data,[8b-c] and because the electronic properties are similarly influenced by the backbone substitution in IMes and IPr ligands series. In supplement to the rhodium complexes $\mathbf{8}^{NMe_2}$ and $\mathbf{8}^{(NMe_2)_2}$ we already described,[14a] the new complex $\mathbf{8}^{NiPr_2}$ was synthesized in two steps from $[RhCl(COD)]_2$ and the corresponding imidazolium salt $\mathbf{3a}^{NiPr_2}$ to give first the intermediate complex $[RhCl(COD)(IMes^{NiPr_2})]$ $\mathbf{7}^{NiPr_2}$ that was converted to the carbonyl complex $\mathbf{8}^{NiPr_2}$ in a subsequent carbonylation step (73% overall yield) (Scheme 2, left side). Taking again advantage of the specific reactivity of the enamine-type heterocyclic backbone of coordinated $IMes^{NMe_2}$, complex $\mathbf{8}^{NMe_2}$ was readily derivatized into $\mathbf{8}^{(NMe_2,Cl)}$ upon reaction with NCS in $CHCl_3$ (Scheme 2, left side).

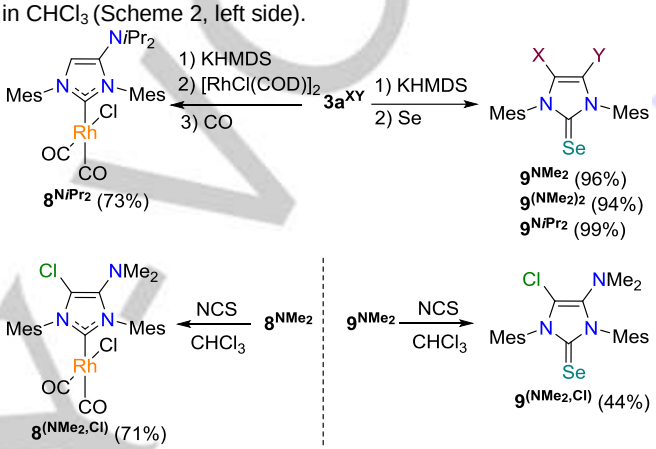

Scheme 2. Synthesis of the new rhodium-carbonyl complexes $\mathbf{8}^{NiPr_2}$ and $\mathbf{8}^{(NMe_2,Cl)}$ and selenoureas $\mathbf{9}^{XY}$.

The π-acidity of the series of NHC ligands we considered was next evaluated against the chemical shifts of the ^{77}Se nuclei in the seleno adducts $IMes^{XY}$-Se, the latter values offering a reliable scale of the π-acidity of NHCs.[23] Here, the new selenoureas $\mathbf{9}^{NMe_2}$ $\mathbf{9}^{(NMe_2)_2}$, and $\mathbf{9}^{NiPr_2}$ were readily synthesized upon reaction of the corresponding carbenes with elemental selenium, while $\mathbf{9}^{(NMe_2,\ Cl)}$ was obtained upon derivatisation of $\mathbf{9}^{NMe_2}$ by reaction with NCS (Scheme 2, right side).

Finally, the steric properties of the ligands in complexes Pd-PEPPSI-NHC $\mathbf{5}^{XY}$ and **6** were quantified by calculating the percent buried volume ($\%V_{bur}$) using the geometry resulting from single crystal X-ray diffraction analyses.[24] Data for complexes $\mathbf{5}^{NMe_2}$ and $\mathbf{5}^{(NMe_2)_2}$ were retrieved from our previous publication,[14a] while those of complexes **5** and **6** were recovered from the CCDC database.[25] Finally, for the fate of comparison, we determined the solid-state structure of complex $\mathbf{5}^{Cl_2}$, which had not been reported before.(Figure S2).

The stereoelectronic parameters of backbone-substituted IPr^{XY} thus determined, along with those of IPent, are gathered in Table 1.

10.1002/chem.201702859

Table 1. Stereoelectronic parameters of backbone-substituted IPr^{XY} and IPent.

Entry	NHC	ν_{CO}^{av} of **8^{XY}** (cm^{-1})[a]	TEP value (cm^{-1})[b]	$\delta(^{77}Se)$ in **9^{XY}** (ppm)[c]	%V_{bur} (%) (from **5^{XY}**)
1	IMes/IPr	2037.6	2050.3	27[d]	34.3
2	(IMes/IPr)^{NMe2}	2035.8	2048.8	32	39.7
3	(IMes/IPr)$^{(NMe2)2}$	2034.0	2047.4	26	40.2/ 38.7
4	(IMes/IPr)^{NiPr2}	2035.0	2048.2	36	40.6
5	(IMes/IPr)$^{(NMe2,Cl)}$	2038.0	2050.6	68	39.8
6	(IMes/IPr)^{Cl2}	2042.5	2054.2	174[f]	34.2
7	IPent	-	2049.3[e]	101[d]	38.3

[a] IR spectra recorded in CH_2Cl_2; [b] TEP values calculated using the equation TEP = 0.8001 ν_{CO}^{av} + 420.0 cm^{-1}; [c] NMR spectra recorded in $CDCl_3$; [d] from reference 23b; [e] from reference 26; [f] Value obtained from IPr^{Cl2}, from reference 23b.

Several features can be drawn from a detailed analysis of these data. First, the ^{77}Se chemical shifts of the amino-substituted NHC-Se adducts **9^{NMe2}**, **9$^{(NMe2)2}$** and **9^{NiPr2}** do not really differ from the one of the unsubstituted derivative **9**, highlighting that the grafting of an amino group onto the imidazolyl skeleton has only little effect, if any, on the π-acidity of the corresponding NHC (entries 1-4). In other words, the amino groups interact at best weakly with the π-system of the imidazol-2-ylidene. This corroborates our recent work on amino/ammonio-substituted imidazol-2-ylidenes and is in agreement with previous DFT calculations by Huber and Weiss on related systems.[27,28] Comparison of the TEP values confirms our working hypothesis as a size increase of the amino group does not affect the electron donicity of the mono-substituted NHCs (compare **8^{NMe2}** vs. **8^{NiPr2}**, entries 2 and 4), whereas the formal substitution of a dimethylamino group in **8$^{(NMe2)2}$** by a chloride led to a diminished electronic donation of the chloro-amino-substituted NHC in **8$^{(NMe2,Cl)}$** (entries 3 and 5). Interestingly, the TEP value of the latter NHC is about the same as the unsubstituted standard IMes ligand. Yet the %V_{bur} of IPr$^{(NMe2,Cl)}$ ligand in **5$^{(NMe2,Cl)}$** (entry 5) is much higher than the one of standard IPr in **5** (entry 1), and is similar to the one of IPr$^{(NMe2)2}$ in **5$^{(NMe2)2}$** (entry 3). Actually, it appears that the substitution of the heterocyclic backbone by at least one amino group leads to a strong increase of the %V_{bur} from 34.3% in **5** (entry 1) to values around 40% in **5^{NMe2}**, **5$^{(NMe2)2}$**, **5^{NiPr2}**, and **5$^{(NMe2,Cl)}$** (entries 2-5). As expected, the substitution of the heterocycle by two chlorine atoms gives access to a poorer electron donating NHC, but this has virtually no effect on the steric shielding of the IPr^{Cl2} ligand in complex **5^{Cl2}** compared to **5**.

Correlating the stereoelectronic properties of the NHCs with the catalytic activity of the corresponding pre-catalysts **5^{XY}** allows to conclude that the beneficial effect observed with amino-substituted IPr ligands is steric in origin and that electronic effects are much less important. This is particularly clear when considering the catalytic activity of pre-catalyst **5$^{(NMe2,Cl)}$**, which is about the same as the of **5$^{(NMe2)2}$**, while IPr$^{(NMe2,Cl)}$ is much less electron-donating than IPr$^{(NMe2)2}$. Conversely, the carbenes IPr^{NiPr2} and IPr^{NMe2} exhibit about the same electron donating properties, but **5^{NiPr2}** greatly surpasses **5^{NMe2}** in terms of efficiency in amination catalysis. At that point, we could not totally figure the exact, precise effect the backbone substituents had on the catalytic activity of the resulting complexes since the %V_{bur} is a global steric descriptor, and the %V_{bur} for the four amino-substituted IPr ligands we considered are very close and should actually be considered as identical within the experimental errors. Opportunely, in 2016 Cavallo and co-workers put the new SambVca2 web application at disposal of the research community.[29] The implementation of the X-Ray structures of complexes **5**, **5^{XY}**, and **6** into this application gave access to the three-dimensional topographical map of our complexes. The shape of the catalytic pocket defined by the ancillary NHC ligand could then be analyzed in details. By choosing the right coordinates, the coordination sphere around Pd was divided into four quadrants and the steric shielding provided by the NHC ligands in each of them was calculated separately. The $C_{carbene}$-Pd bond was chosen as the z axis and the imidazolylidene plane constituted the (xz) plane. With this cutting, each quadrant is occupied by one of the four *ortho* substitutents of the N-aryl groups of the NHC ligand (*i*Pr group for complexes **5^{XY}** and 3-pentyl group for complex **6**) (Figure 5).

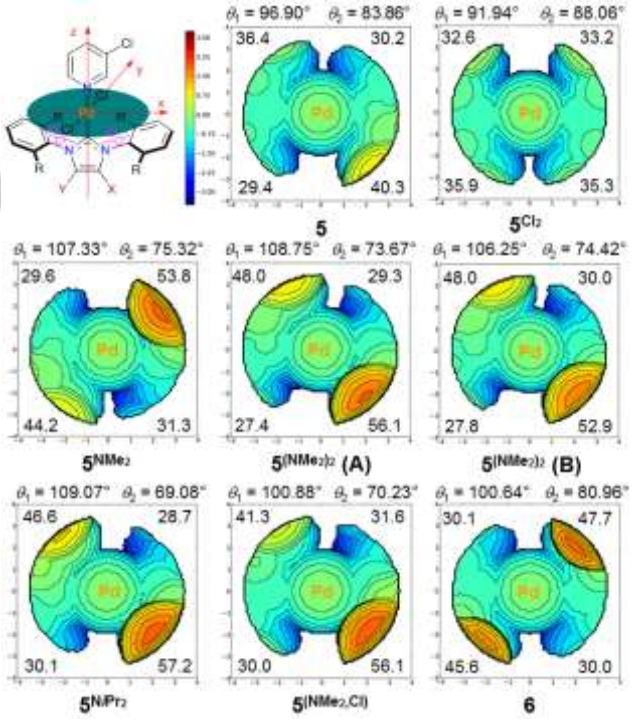

Figure 5. Steric map views of the Pd-PEPPSI-NHC complexes **5^{XY}** and **6**. For unsymmetrically substituted complexes, the amino group was placed arbitrarily as the X substituent and was thus on the right of the steric map. θ_1 and θ_2

10.1002/chem.201702859

represent the dihedral angles between the imidazolyl and aryl planes. Values in corners are the %V_{bur} of the NHC ligand in the corresponding quadrant.

In general, except for complex **5**^{Cl_2}, two diametrically opposed quadrants are sterically crowded, whereas the other two are relatively unhindered. Noteworthy, the most hindered quadrant is always on the same side as the amino group on the heterocyclic backbone (on the right side of the steric map), confirming that the NMe_2 and the N*i*Pr_2 groups clearly push one of the *ortho*-*i*Pr groups of the Dipp aryl groups in direction of the reactive catalytic site. This is done through a twist of the aryl group around the N-C_{Dipp} bond illustrated by the dihedral angles θ_1 and θ_2, which largely deviate from 90°. They also exert a repulsion directly on the isopropyl group and force the latter to interact more tightly with the palladium center. Such an additional repulsion is clear in complex **5**^{NMe_2}, in which the more steric quadrant is on the NMe_2 side (North-East quadrant: 53.8%), whereas the dihedral angle θ_1 = 72.67° is more acute than θ_2 = 75.32°. On the overall, the %V_{bur} values in the bulky quadrants and the asymmetry level between the four quadrants are positively correlated with the respective catalytic activities of the pre-catalysts **5**^{XY}. For example, the most active catalysts **5**$^{(NMe_2)_2}$, **5**$^{(NMe_2,Cl)}$, and **5**^{NiPr_2} are the most dissymmetric and exhibit the most highly congested quadrants. Interestingly, complex **5**$^{(NMe_2)_2}$ is represented by two independent conformers in the crystal lattice with conformer **A** being more crowded than conformer **B**, thus indicating that the bulky IPr$^{(NMe_2)_2}$ ligand nevertheless possesses some degree of flexibility. Concerning the mechanism of the amination reactions, the dependence of the catalytic efficiency against the steric properties of the NHC ligands would support a catalytic cycle in which the rate limiting step is the reductive elimination step. Indeed, it is well accepted that the latter is facilitated by the increase of the bulkiness of the supporting ligand, while the oxidative addition step and the coordination-deprotonation of the amine are much less affected by the steric hindrance.

We attribute the beneficial influence of the carbenic heterocycle decoration to a buttressing effect of the amino groups. The concept of buttressing effect was first introduced to rationalize some long range interactions between substituents in aryl chemistry: the effect of a substituent in *ortho* position of a defined functional group is strengthened by the presence of another more distant group, usually on the *meta* position.[30] This effect can influence the conformational dynamic, the thermodynamic properties such as acidity and basicity, or the reactivity of the functional group.[31] Tomioka introduced this concept in reactive triplet carbene chemistry, where the *meta* alkyl substituent R forces the methyl group of the OMe substituent to be out the plane of the aryl group and thus to interact more efficiently with the carbene center in a C-H bond insertion reaction (Scheme 3A).[32] Here, the amino groups on the 4 and/or 5 position of the imidazolyl ring forces *the twist* of the 2,6-diisopropylphenyl groups around the N-C bond from the orthogonal starting conformation, which induces a more closely interaction of the *i*Pr groups with the active coordination sphere (Scheme 3B). We thus propose that the key design principle in the backbone decoration of our NHCs for Pd-catalyzed amination reaction rests on the buttressing effect of the amino substituents. As an extension, this study would also provide a rationalization of the beneficial effect that previous NHC-backbone substitution had in the Buchwald-Hartwig amination reaction.[15,17]

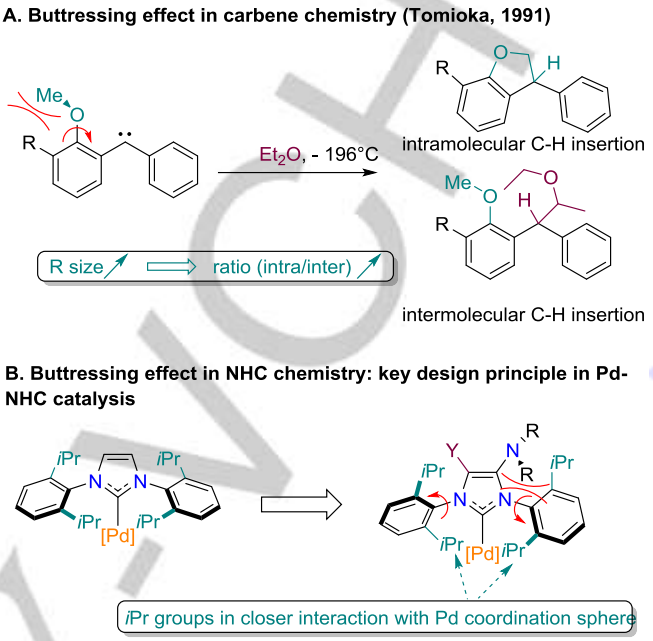

Scheme 3. Buttressing effect in carbene chemistry (**A**) and in NHC-Pd catalysis (**B**).

Implementation of buttressing effect in Pd-catalyzed arylation of bulky primary amines

In order to further illustrate the usefulness and versatility of this approach, we devised developing a challenging amination reaction with our ligand set and we focused on the arylation of very hindered α,α,α-trisubstituted primary amines. Despite the broad interest of incorporating bulky alkyl groups in compounds of pharmaceutical interest,[33] the Buchwald-Hartwig amination reaction using bulky primary amines such as *tert*-butylamine or 1-adamantyl amine had been barely studied. The catalytic systems that have been disclosed generally suffer from quite high catalyst loading (1-5 mol%), high reaction temperatures (100-120°C), and the scope was often restricted to one or two examples.[34,35] Still, in 2015, Buchwald and co-workers reported a very efficient phosphine-based catalytic system operating under relatively mild conditions (0.5-2 mol% of catalyst, NaO*t*Bu as base, reaction temperature: 80-120°C) and exhibiting a very wide substrate scope.[37]

The highly challenging coupling between 2-chloroanisole and *tert*-butylamine - never reported to date - was chosen as model reaction. Potassium *tert*-butoxide and DME were selected as base and solvent, respectively, and we decided to operate at the quite low temperature of 60°C to have the reaction conditions as mild as possible (Table 2). In an initial screening, the efficiencies of pre-catalysts **5**$^{(NMe_2)_2}$, **5**^{NiPr_2}, and **5**$^{(NMe_2,Cl)}$, which were the most active pre-catalysts in the previous study (Figures 3 and 4), were evaluated. Disappointingly, the best conversion we got was 30% only after 4 h using **5**^{NiPr_2}, whereas pre-catalysts **5**$^{(NMe_2)_2}$ and

10.1002/chem.201702859

FULL PAPER

5$^{(NMe_2,Cl)}$ were almost inactive under these conditions (Table 2, entries 1-3).

Table 2. Screening of pre-catalysts **5^{XY}**, **11^{XY}** and **12** and reaction conditions for the arylation of *tert*-butyl amine with 2-chloroanisole.[a]

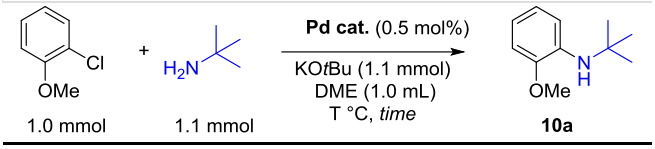

Entry	Pd cat.	T (°C)	time (h)	GC conv. (%)[b]
1	**5$^{(NMe2)2}$**	60	4	5
2	**5^{NiPr2}**	60	4	30
3	**5$^{(NMe2,Cl)}$**	60	4	traces
4	**11$^{(NMe2)2}$**	60	1	100
5	**11^{NiPr2}**	60	2	95
6	**11$^{(NMe2,Cl)}$**	60	4	15
7	**11^{NMe2}**	60	4	84
8	**11**	60	3	0 (5)[c]
9	**11$^{(NMe2)2}$**	40	3	97
10	**11^{NiPr2}**	40	3	87
11	**12**[d]	40	3	88

[a] Reaction conditions: 2-chloroanisole (1.0 mmol), *tert*-butylamine (1.1 mmol), Pd cat. (0.5 mol%), KO*t*Bu (1.1 mmol), DME (1.0 mL). [b] Calibrated GC conversions were reported using dodecane as the internal standard and were averaged over two runs. [c] Conversion in parentheses after 24 h of reaction. [d] **12** = PdCl(cin)(IPent).

We assigned this lack of activity to a sluggish activation of the pre-catalysts to form the [Pd^0(NHC)] active species. Indeed, the Pd-PEPPSI-NHC type catalysts are known to be readily reduced to Pd^0 species when using morpholine and KO*t*Bu through displacement of the pyridine by morpholine, deprotonation to generate an amido-complex, β-hydrogen elimination, and reductive elimination of HCl from [(NHC)PdClH] species.[10b,38] Here, *tert*-butylamine does not possess β-hydrogens, which severely hinders the activation pathway. We thus reasoned that a pre-catalyst known to be more readily activated by a base would circumvent this issue. As the [PdCl(cin)(NHC)] complexes, first disclosed by Nolan,[15a] were proved to be readily activated by bases such as KO*t*Bu through a nucleophilic attack of the latter on the cinnamyl ligand, we synthesized the series of pre-catalysts **11^{NMe_2}**, **11$^{(NMe_2)_2}$**, and **11^{NiPr_2}** by reacting the *in situ* generated free NHC with [PdCl(cin)]$_2$ (Scheme 4). In addition, using our chlorination strategy, **11$^{(NMe_2,Cl)}$** was obtained in high yield by reacting **11^{NMe_2}** with NCS in $CHCl_3$. All complexes were obtained in analytically pure form and the molecular structures of **11^{NMe_2}** and **11$^{(NMe_2,Cl)}$** were confirmed by X-Ray diffraction analysis (Figures S3 and S4 in the ESI).

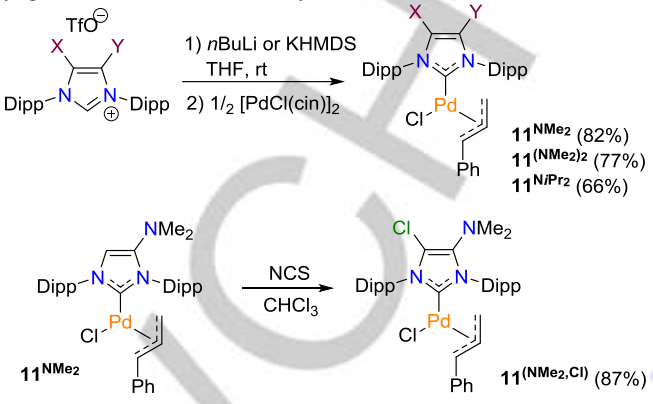

Scheme 4. Synthesis of the new [PdCl(cin)(IPr^{XY})] pre-catalysts **11^{XY}**.

Gratifyingly, complexes **11$^{(NMe_2)_2}$** and **11^{NiPr_2}** were found to be highly efficient in the model reaction. Full conversion is observed after 1 hour at 60°C for **11$^{(NMe_2)_2}$** while complex **11^{NiPr_2}** leads to 95% conversion after 2 hours (Table 2, entries 4-5). Surprisingly, complex **11$^{(NMe_2,Cl)}$** gives 15% conversion only under the same conditions (entry 6). We tentatively assigned this discrepancy to a low stability of the catalyst in this case. Pre-catalyst **11^{NMe_2}** bearing the less bulky IPr^{NMe_2} ligand is a little less efficient with 84% conversion after 4 hours, while the standard pre-catalyst [PdCl(cin)(IPr)] (**11**) leads to almost no conversion (entries 7-8). Strikingly, the catalysis could even be carried out at 40°C with pre-catalysts **11$^{(NMe_2)_2}$** and **11^{NiPr_2}** with only a slight alteration of the conversion (97% using **11$^{(NMe_2)_2}$** and 87% using **11^{NiPr_2}** after 3 hours, entries 9-10). Eventually, under the same reaction conditions, the complex [PdCl(cin)(IPent)] (**12**) exhibits about the same activity as complex **11^{NiPr_2}** (entry 11).

With the fully optimized catalytic conditions in hand, the substrate scope was next investigated with respect to the nature of the bulky amine and of the stereoelectronic properties of the (hetero)aryl chloride partner (Scheme 5). Under these mild reactions conditions, pre-catalyst **11$^{(NMe_2)_2}$** is highly efficient for the coupling of *tert*-butylamine or 1-adamantylamine with a wide range of *ortho* *meta* or *para* substituted aryl chlorides, eventually possessing strongly deactivating methoxy groups, as well as with heteroaryl and naphthyl derivatives, to afford the coupling products **10a-i** in excellent yields and short reaction time. Although a slightly higher reaction temperature (60°C) is required in certain cases for achieving good conversions when using adamantyl amine (**10g-i**), the conditions employed here generally remain much milder than the ones previously reported in literature.[34-37] These encouraging results prompted us to further explore the possibility to couple even more sterically hindered amines such as *tert*-amyl amine, *tert*-octyl amine, and trityl amine, which appeared to be suitable substrates in Pd-catalyzed amination only recently.[37] For these amines, the temperature of 60°C was found necessary to achieve a good conversion. Interestingly, complex **11^{NiPr_2}** performed systematically better than **11$^{(NMe_2)_2}$** for coupling *t*-amyl

10.1002/chem.201702859

amine and *t*-octyl amines. For instance, full conversion is observed for the coupling of 2-chloroanisole and t-octyl amine with **11**^{NiPr_2} after 4 hours at 60°C to afford **10k**, while a 84% conversion only is obtained when using **11**$^{(NMe_2)_2}$. The higher flexibility of IPr^{NiPr_2} ligand compared to IPr$^{(NMe_2)_2}$ may be a reasonable explanation for this trend, allowing the ligand to better accommodate the very high steric hindrance of the amine substrate. A variety of challenging (hetero)aryl chlorides can also be successfully engaged in this reaction to afford the coupling products **10j-o** and **10q** using 0.5 mol% of **11**^{NiPr_2}. An increase of the catalyst loading to 1 mol% and reaction time to 18 h are needed to produce **10p** albeit in an excellent 99% isolated yield. Strikingly, using 1 mol% of catalyst **11**$^{(NMe_2)_2}$, trityl amine can even be successfully coupled with 4-chloro and 2-chloroanisole to give **10r-s** in 82%, and 83% yields, respectively. Coupling of the latter with 3-chloropyridine is a little less efficient but **10t** is nevertheless obtained in 54% yield. Turning now our attention to the di-ortho substituted aryl chlorides, we found that 2-chloroxylene can be readily coupled with adamantyl amine, *t*-amyl amine and *t*-octyl amine to give anilines **10u-w** using 1 mol% of **11**$^{(NMe_2)_2}$ (2 mol% for **10w**) at 60°C for a longer but still acceptable time of 14-18 h. Under the same reaction conditions, complex **11**^{NiPr_2} is much less efficient and we explain this fact by a lower catalyst stability. Finally, 2,6-dimethoxyphenyl chloride is a suitable substrate producing anilines **10x-y** in good yields.

Conclusions

Prompted by the huge impact of the Pd-catalyzed arylative amination in synthetic chemistry, the quest of improved Pd-NHC catalysts has been the subject of intense research over the last decade and major breakthroughs have often been attained by advances in ligand design. While earlier successful developments mainly relied on the modification of the N-aryl groups, the recent years have seen the advent of a complementary strategy based on the direct decoration of the carbenic heterocycle. We have now demonstrated in the case of amino and chloro substituted IPr derivatives that the beneficial effect of the substitution observed in catalysis can be correlated to the stereoelectronic features of the ligand. In particular, the amino groups, and to a lower extent the chloro substituents, exert a steric constrain on the Dipp arms forcing them to be twisted and to interact more strongly with the coordination sphere during the catalytic process. This relay ensured by the N-Dipp groups is very similar to the well-known buttressing effect occurring in aromatic compounds. This buttressing effect thus appears as the key leading principle in the optimization of NHC ligands by substitution of their heterocyclic backbones and would serve as a rationalizing frame for the observed beneficial influence of the NHC-backbone decoration.
Thanks to the non-spherical tridimensional structure of the amino groups NR_2, which can accommodate several conformations, this steric effect does not rigidify too much the system and some flexibility degree remains present, the latter being necessary for a better catalyst efficiency. We further validated the potential of our ligand design strategy by implementing a proper ligand set in the challenging arylation of highly sterically hindered α,α,α-trisubstituted primary amines using aryl chlorides as electrophilic partners.

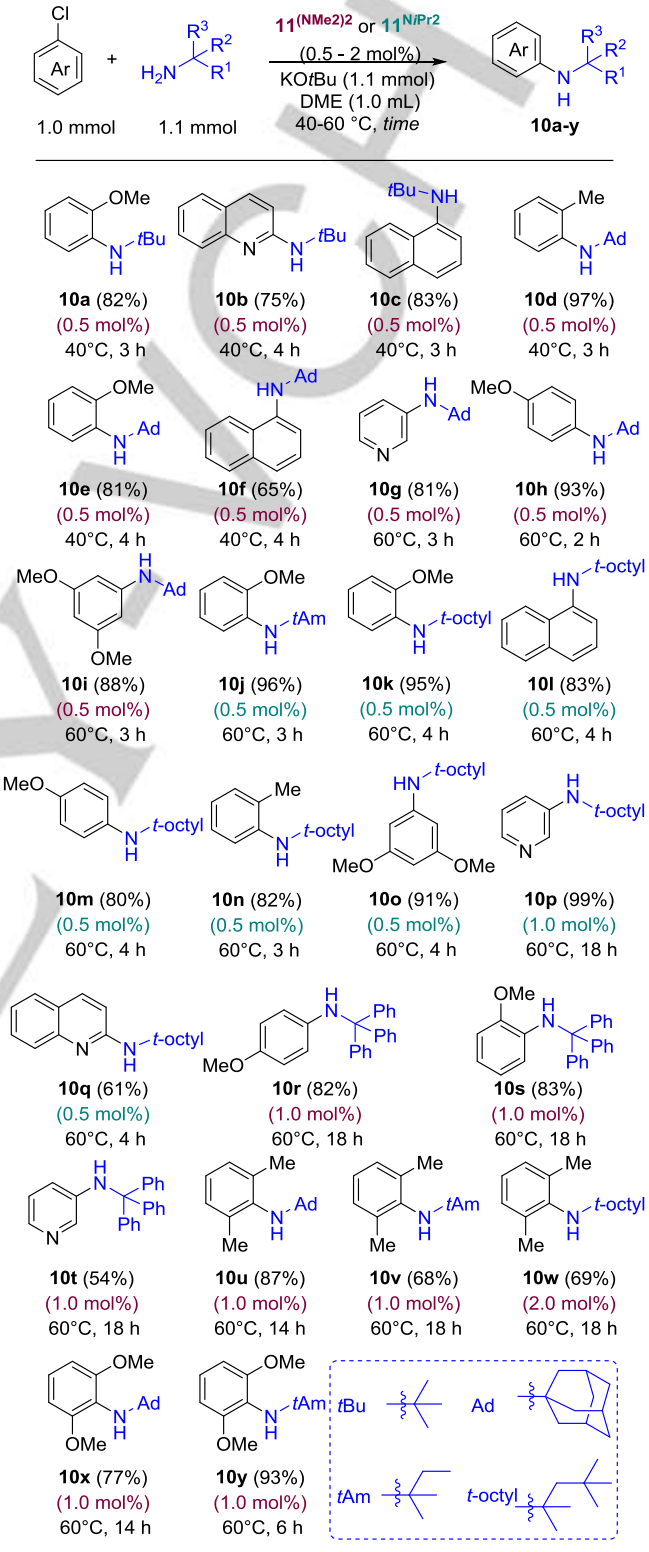

Scheme 5. Scope of the Pd-catalyzed arylation of bulky primary amines using pre-catalysts **11**$^{(NMe_2)_2}$ or **11**^{NiPr_2} , yields refer to the average of isolated yields of two runs after column chromatography. Reaction conditions: aryl chloride (1.0 mmol), amine (1.1 mmol), KO*t*Bu (1.1 mmol), DME (1.0 mL).

Here again, besides a judicious choice of the pre-catalyst type, the buttressing effect of the backbone substituents appeared decisive for the generation of highly efficient catalysts, with the pre-catalysts [PdCl(cin)(IPr^{NiPr2})] and [PdCl(cin)(IPr$^{(NMe2)2}$] being the most efficient ones. Noteworthy, the catalytic conditions are unprecedentedly mild, since catalyst loadings of 0.5-2 mol% and reaction temperatures between 40 and 60°C are sufficient to couple a large variety of aryl chlorides and bulky primary amines. We are currently working on the extension of this ligand design principle in other metal-NHC catalyzed reactions.

Acknowledgements

This work was supported by the "Centre National de la Recherche Scientifique" (CNRS). We are grateful to the China Scholarship Council for providing a PhD grant to Yin Zhang. Dr Christian Bijani (LCC-CNRS) is warmly acknowledged for his help with the ^{77}Se NMR.

Keywords: N-heterocyclic carbenes • ligand design • palladium • catalysis • C-N bond • primary amines

[1] Recent book chapter: J. Paradies, in *Metal-Catalyzed Cross-Coupling Reactions and More* (Eds: A. de Meijere, S. Bräse, M. Oestreich), Wiley-VCH, **2014**, pp. 995-1066.

[2] Selected recent reviews: (a) P. Ruiz-Castillo, S. L. Buchwald, *Chem. Rev.* **2016**, *116*, 12564-12649; (b) J. Bariwal, E. Van der Eycken, *Chem. Soc. Rev.* **2013**, *42*, 9283-9303; (c) C. Torborg, M. Beller, *Adv. Synth. Catal.* **2009**, *351*, 3027-3043; (d) S. L. Buchwald, C. Mauger, G. Mignani, U. Scholz, *Adv. Synth. Catal.* **2006**, *348*, 23-39; (e) S. L. Buchwald, C. Mauger, G. Mignani, U. Scholz, *Adv. Synth. Catal.* **2006**, *348*, 23-39.

[3] (a) P. G. Gildner, T. J. Colacot, *Organometallics* **2015**, *34*, 5497-5508; (b) H. Li, C. C. C. Johansson Seechurn, T. J. Colacot, *ACS Catal.* **2012**, *2*, 1147-1164.

[4] (a) D. S. Surry, S. L. Buchwald, *Chem. Sci.* **2011**, *2*, 27-50; (b) C. A. Fleckenstein, H. Plenio, *Chem. Soc. Rev*. **2010**, *39*, 694-711; (c) J. F. Hartwig, *Acc. Chem. Res.* **2008**, *41*, 1534-1544.

[5] For monographs on NHC chemistry, see: (a) *N-Heterocyclic Carbenes: Effective Tools for Organometallic Synthesis* (Ed.: S. P. Nolan), Wiley-VCH, Weinheim, **2014**; (b) *N-Heterocyclic Carbenes* (Ed.: S. Díez-González), RSC, Cambridge (UK), **2011**; (c) C. S. J. Cazin, *N-Heterocyclic Carbenes in Transition Metal Catalysis and Organocatalysis. In Catalysis by Metal Complexes*, Vol. 32, Springer, Berlin (Germany), **2011**.

[6] For general reviews on NHCs, see: (a) M. N. Hopkinson, C. Richter, M. Schedler, F. Glorius, *Nature* **2014**, *510*, 485-496; (b) D. Bourissou, O. Guerret, F. P. Gabbai, G. Bertrand, *Chem. Rev.* **2000**, *100*, 39-92. NHCs in organometallic catalysis: (c) S. Bellemin-Laponnaz, S. Dagorne, *Chem. Rev.* **2014**, *114*, 8747-8774; (d) K. Riener, S. Haslinger, A. Raba, M. P. Högerl, M. Cokoja, W. A. Herrmann, F. E. Kühn, *Chem. Rev.* **2014**, *114*, 5215-5272; (e) S. Díez-González, N. Marion, S. P. Nolan, *Chem. Rev.* **2009**, *109*, 3612-3676.

[7] For Pd-NHC complexes in palladium-catalyzed cross-coupling reactions, see: (a) C. Valente, S. Çalimsiz, K. H. Hoi, D. Mallik, M. Sayah, M. G. Organ, *Angew. Chem. Int. Ed.* **2012**, *51*, 3314-3332; (b) G. C. Fortman, S. P. Nolan, *Chem. Soc. Rev.* **2011**, *40*, 5151-5169.

[8] (a) L. Benhamou, E. Chardon, G. Lavigne, S. Bellemin-Laponnaz, V. César, *Chem. Rev.* **2011**, *111*, 2705-2733; (b) D. J. Nelson, S. P. Nolan *Chem. Soc. Rev.* **2013**, *42*, 6723-6753; (c) T. Dröge, F. Glorius, *Angew. Chem. Int. Ed.* **2010**, *49*, 6940-6952.

[9] For earlier reports on Pd-IPr systems, see: (a) M. G. Organ, M. Abdel-Hadi, S. Avola, I. Dubovyk, N. Hadei, E. A. B. Kantchev, C. J. O'Brien, M. Sayah, C. Valente, *Chem. Eur. J.* **2008**, *14*, 2443-2452; (b) N. Marion, E. C. Ecarnot, O. Navarro, D. Amoroso, A. Bell, S. P. Nolan, *J. Org. Chem.* **2006**, *71*, 3816-3821; (c) O. Navarro, H. Kaur, P. Mahjoor, S. P. Nolan, *J. Org. Chem.* **2004**, *69*, 3173-3180.

[10] (a) K. H. Hoi, S. Çalimsiz, R. D. J. Froese, A. C. Hopkinson, M. G. Organ, *Chem. Eur. J.* **2011**, *17*, 3086-3090; (b) K. H. Hoi, S. Çalimsiz, R. D. J. Froese, A. C. Hopkinson, M. G. Organ, *Chem. Eur. J.* **2012**, *18*, 145-151.

[11] (a) S. Meiries, G. Le Duc, A. Chartoire, A. Collado, K. Speck, K. S. A. Arachchige, A. M. Z. Slawin, S. P. Nolan, *Chem. Eur. J.* **2013**, *19*, 17358-17368; (b) E. Marelli, A. Chartoire, G. Le Duc, S. P. Nolan, *ChemCatChem* **2015**, *7*, 4021-4024.

[12] (a) F. Izquierdo, S. Manzini, S. P. Nolan, *Chem. Commun.* **2014**, *50*, 14926-14937; (b) G. Bastug, S. P. Nolan, *Organometallics* **2014**, *33*, 1253-1258; (c) S. Meiries, A. Chartoire, A. M. Z. Slawin, S. P. Nolan, *Organometallics* **2012**, *31*, 3402-3409; (d) A. Chartoire, X. Frogneux, A. Boreux, A. M. Z. Slawin, S. P. Nolan, *Organometallics* **2012**, *31*, 6947-6951.

[13] (a) S. Würtz, F. Glorius, *Acc. Chem. Res.* **2008**, *41*, 1523-1533; (b) G. Altenhoff, R. Goddard, C. W. Lehmann, F. Glorius, *J. Am. Chem. Soc.* **2004**, *126*, 15195-15201; (c) G. Altenhoff, R. Goddard, C. W. Lehmann, F. Glorius, *Angew. Chem. Int. Ed.* **2003**, *42*, 3690-3693.

[14] For contributions of our group, see: (a) Y. Zhang, V. César, G. Storch, N. Lugan, G. Lavigne, *Angew. Chem. Int. Ed.* **2014**, *53*, 6482-6486; (b) Y. Zhang, V. César, G. Lavigne, *Eur. J. Org. Chem.* **2015**, 2042-2050; (c) Y. Zhang, G. Lavigne, V. César, *J. Org. Chem.* **2015**, *80*, 7666-7673; See also: (d) V. César, Y. Zhang, W. Kośnik, A. Zieliński, A. A. Rajkiewicz M. Ruamps, S. Bastin, N. Lugan, G. Lavigne, K. Grela, *Chem. Eur. J.* **2017**, *23*, 1950-1955.

[15] For other contributions, see: (a) N. Marion, O. Navarro, J. Mei, E. D. Stevens, N. M. Scott, S. P. Nolan, *J. Am. Chem. Soc.* **2006**, *128*, 4101-4111; (b) T. Tu, W. Fang, J. Jiang, *Chem. Commun.* **2011**, *47*, 12358-12360; (c) T. Tu, Z. Sun, W. Fang, M. Xu, Y. Zhou, *Org. Lett.* **2012**, *14*, 4250-4253; (d) W. Fang, J. Jiang, Y. Xu, J. Zhou, T. Tu, *Tetrahedron* **2013**, *69*, 673-679; (e) A. Winkler, K. Brandhorst, M. Freytag, P. G. Jones M. Tamm, *Organometallics* **2016**, *35*, 1160-1169; (f) X.-B. Lan, F.-M. Chen, B.-B. Ma, D.-S. Shen, F.-S. Liu, *Organometallics* **2016**, *35*, 3852-3860; (g) A. Rühling, L. Rakers, F. Glorius, *ChemCatChem* **2017**, *9*, 547-550.

[16] PEPPSI = Pyridine-Enhanced Pre-Catalyst Preparation, Purification, Stabilization and Initiation.

[17] For the use of IPent^{Cl2} and IHept^{Cl2} in Buchwald-Hartwig amination, see: (a) K. H. Hoi, J. A. Coggan, M. G. Organ, *Chem. Eur. J.* **2013**, *19*, 843-845; (b) C. Valente, M. Pompeo, M. Sayah, M. G. Organ, *Org. Process. Res. Dev.* **2013**, *18*, 180-190; (c) M. Pompeo, J. L. Farmer, R. D. J. Froese, M. G. Organ, *Angew. Chem. Int. Ed.* **2014**, *53*, 3223-3226; (d) S. Sharif, R. P. Rucker, N. Chandrasoma, D. Mitchell, M. J. Rodriguez, R. D. J. Froese, M. G. Organ, *Angew. Chem. Int. Ed.* **2015**, *54*, 9507-9511; (e) C. Lombardi, J. Day, N. Chandrasoma, D. Mitchell, M. J. Rodriguez, J. L. Farmer, M. G. Organ, *Organometallics* **2017**, *36*, 251-254; (f) A. Khadra, S. Mayer, M. G. Organ, *Chem. Eur. J.* **2017**, *23*, 3206-3212.

[18] For the use of IPent^{Cl2} and IHept^{Cl2} in other Pd-catalyzed cross-coupling reactions, see: (a) B. Atwater, N. Chandrasoma, D. Mitchell, M. J. Rodriguez, M. G. Organ, *Chem. Eur. J.* **2016**, *22*, 14531-14534; (b) B. Atwater, N. Chandrasoma, D. Mitchell, M. J. Rodriguez, M. Pompeo, R. D. J. Froese, M. G. Organ, *Angew. Chem. Int. Ed.* **2015**, *54*, 9502-9506; (c) M. Sayah, M. G. Organ, *Chem. Eur. J.* **2013**, *19*, 16196-16199; (d) M. Sayah, A. J. Lough, M. G. Organ *Chem. Eur. J.* **2013**, *19*, 2749-2756; (e) M. Pompeo, R. D. J. Froese, N. Hadei, M. G. Organ, *Angew. Chem. Int. Ed.* **2012**, *51*, 11354-11357.

[19] (a) V. César, V. Mallardo, A. Nano, G. Dahm, N. Lugan, G. Lavigne, S. Bellemin-Laponnaz, *Chem. Commun.* **2015**, *51*, 5271-5274; (b) V. César, J.-C. Tourneux, N. Vujkovic, R. Brousses, N. Lugan, G. Lavigne, *Chem. Commun.* **2012**, *48*, 2349-2351; (c) L. Benhamou, N. Vujkovic, V. César,

H. Gornitzka, N. Lugan, G. Lavigne, *Organometallics* **2010**, *29*, 2616-2630; (d) L. Benhamou, V. César, H. Gornitzka, N. Lugan, G. Lavigne, *Chem. Commun.* **2009**, 4720-4722.

[20] (a) D. Mendoza-Espinosa, B. Donnadieu, G. Bertrand, *J. Am. Chem. Soc.* **2010**, *132*, 7264-7265; (b) M. L. Cole, C. Jones, P. C. Junk, *New J. Chem.* **2002**, *26*, 1296-1303; (c) A. J. Arduengo, F. Davidson, H. V. R. Dias, J. R. Goerlich, D. Khasnis, W. J. Marshall, T. K. Prakasha, *J. Am. Chem. Soc.* **1997**, *119*, 12742-12749.

[21] V. César, N. Lugan, G. Lavigne, *Chem. Eur. J.* **2010**, *16*, 11432-11442.

[22] (a) R. A. Kelly III, H. Clavier, S. Giudice, N. M. Scott, E. D. Stevens, J. Bordner, I. Samardjiev, C. D. Hoff, L. Cavallo, S. P. Nolan, *Organometallics* **2007**, *27*, 202-210; (b) S. Wolf, H. Plenio, *J. Organomet. Chem.* **2009**, *694*, 1487-1492.

[23] (a) K. Verlinden, H. Buhl, W. Frank, C. Ganter, *Eur. J. Inorg. Chem.* **2015**, 2416-2425; (b) S. V. C. Vummaleti, D. J. Nelson, A. Poater, A. Gomez-Suarez, D. B. Cordes, A. M. Z. Slawin, S. P. Nolan, L. Cavallo, *Chem. Sci.* **2015**, *6*, 1895-1904; (c) A. Liske, K. Verlinden, H. Buhl, K. Schaper, C. Ganter, *Organometallics* **2013**, *32*, 5269-5272.

[24] (a) A. Poater, B. Cosenza, A. Correa, S. Giudice, F. Ragone, V. Scarano, L. Cavallo, *Eur. J. Inorg. Chem.* **2009**, 1759-1766; For a review, see: (a) H. Clavier, S. P. Nolan, *Chem. Commun.* **2010**, *46*, 841-861.

[25] Complex **5**: CCDC 761247; Complex **6**: CCDC 718904. The data were obtained free of charge from the Cambridge Crystallographic Data Centre via www.ccdc.cam.ac.uk/data_Information.

[26] A. Collado, J. Balogh, S. Meiries, A. M. Z. Slawin, L. Falivene, L. Cavallo, S. P. Nolan, *Organometallics* **2013**, *32*, 3249-3252.

[27] M. Ruamps, N. Lugan, V. César, *Organometallics* **2017**, *36*, 1049-1055.

[28] S. M. Huber, F. W. Heinemann, P. Audebert, R. Weiss, *Chem. Eur. J.* **2011**, *17*, 13078-13086.

[29] L. Falivene, R. Credendino, A. Poater, A. Petta, L. Serra, R. Oliva, V. Scarano, L. Cavallo, *Organometallics* **2016**, *35*, 2286-2293.

[30] R. Adams, H. C. Yuan, *Chem. Rev*. **1933**, *12*, 261-338.

[31] For selected examples, see: (a) J.-Y. Li, H.-I. Chang, C.-N. Feg, Y.-T. Wu, *Org. Lett.* **2016**, *18*, 6444-6447; (b) A. F. Pozharskii, O. V. Ryabtsova, V. A. Ozeryanskii, A. V. Degtyarev, O. N. Kazheva, G. G. Alexandrov, O. A. Dyachenko, *J. Org. Chem*. **2003**, *68*, 10109-10122; (c) C. Heiss, F. Leroux, M. Schlosser, *Eur. J. Org. Chem.* **2005**, 5242-5247; (d) J. Gorecka, C. Heiss, R. Scopelliti, M. Schlosser, *Org. Lett*. **2004**, *6*, 4591-4593; (e) L. A. Paquette, J. M. Gardlik, *J. Am. Chem. Soc.* **1980**, *102*, 5033-5035; (f) S. L. Chien, R. Adams, *J. Am. Chem. Soc.* **1934**, *56*, 1787-1792.

[32] H. Tomioka, K. Kimoto, H. Murata, Y. Izawa, *J. Chem. Soc. Perkin Trans. 1* **1991**, 471-477.

[33] L. Wanka, K. Iqbal, P. R. Schreiner, *Chem. Rev*. **2013**, *113*, 3516-3604.

[34] Selected phosphine-based systems: (a) A. Dumrath, C. Lübbe, H. Neumann, R. Jackstell, M. Beller, *Chem. Eur. J.* **2011**, *17*, 9599-9604; (b) Q. Shen, T. Ogata, J. F. Hartwig, *J. Am. Chem. Soc*. **2008**, *130*, 6586-6596; (c) A. Ehrentraut, A. Zapf, M. Beller, *J. Mol. Catal. A* **2002**, *182-183*, 515-523; (d) J. P. Wolfe, S. L. Buchwald, *J. Org. Chem*. **2000**, *65*, 1144-1157.

[35] Selected NHC-based systems: (a) refs 15a-b; (b) C. A. Wheaton, J.-P. J. Bow, M. Stradiotto, *Organometallics* **2013**, *32*, 6148-6161.

[36] J. Broggi, H. Clavier, S. P. Nolan, *Organometallics* **2008**, *27*, 5525-5531.

[37] P. Ruiz-Castillo, D. G. Blackmond, S. L. Buchwald, *J. Am. Chem. Soc.* **2015**, *137*, 3085-3092.

[38] J. L. Farmer, M. Pompeo, A. J. Lough, M. G. Organ, *Chem. Eur. J.* **2014**, *20*, 15790-15798.

10.1002/chem.201702859

WILEY-VCH

Layout 1:

FULL PAPER

Buttressed IPr ligand: Through a complete structure/activity study, the dramatic improvement of Pd-NHC catalysts induced by the direct introduction of amino substituents onto the imidazolyl backbone of IPr is shown to be steric in origin, and is the result of the twisting of the N-aryl groups induced by the bulky backbone substituents. The implementation of the strategy in the challenging arylation of α,α,α-trisubstituted primary amines is also reported.

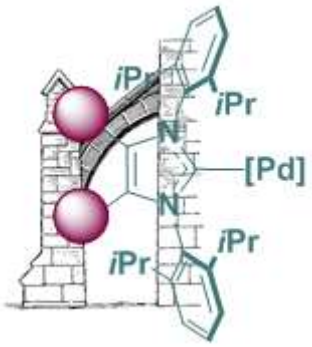

*Yin Zhang, Guy Lavigne, Noël Lugan, Vinecnt César**

Page No. – Page No.
Buttressing effect as key design principle towards highly efficient palladium/N-heterocyclic carbene Buchwald-Hartwig amination catalysts